JOURNAL OF COMPUTATIONAL PHYSICS 38, 265–274 (1980)

Initial Particle Loadings for a Nonuniform Simulation Plasma in a Magnetic Field

H. NAITOU

Institute of Plasma Physics, Nagoya University, Nagoya 464, Japan

S. TOKUDA*

Plasma Physics Laboratory, Faculty of Engineering, Osaka University, Osaka 565, Japan

AND

T. KAMIMURA

Institute of Plasma Physics, Nagoya University, Nagoya 464, Japan

Received September 19, 1978; revised January 18, 1980

Improved methods for initially loading particles in a magnetized simulation plasma with nonuniform density and temperature distributions are proposed. In the usual guiding center loading (GCL), a charge separation coming from finite Larmor radius effects remains because of the difference between the guiding center density and the actual density. The modified guiding center loading (MGCL) presented here eliminates the electric field so generated and can be used for arbitrary density and temperature profiles. Some applications of these methods to actual simulations are given for comparison. The significance of these methods of initial particle loadings is also discussed.

1. INTRODUCTION

With recent increases in simulation techniques and development of electronic computers with faster speeds and larger memories, particle simulation can now treat a rather large-scale plasma in a nonuniform system [1]. However, initial particle loadings for a magnetized, nonuniform plasma have not been studied despite many works using such a plasma.

The difficulty in specifying the initial conditions for a magnetized and nonuniform plasma exists because we cannot explicitly and directly give the actual density distribution. We can only assign the guiding center positions and velocities to simulation particles, following the prescribed equilibrium distribution. The actual positions of the particles are determined automatically by the guiding center positions

* Present address: Japan Atomic Energy Research Institute, Tokai Ibaraki, Japan.

0021-9991/80/150265–10$02.00/0

Copyright © 1980 by Academic Press, Inc.
All rights of reproduction in any form reserved.

and velocities of their particles. The resultant actual density is generally different from the given guiding center density (see, e.g., [2]). If the charge neutrality condition for the guiding center densities is satisfied, which is commonly assumed in the theory and the simulation, then the charge separation for the actual densities remains because of the difference in the average Larmor radii for various particle species. This charge separation excites a large-scale electric field in the inhomogeneous direction, which gives rise to macroscopic plasma flow on the order of the diamagnetic velocity (see Eqs. (11) and (12)). Thus unwanted effects may be added to the phenomena we want to simulate by using the conventional initial condition.

It is important in particle simulations to use initial loadings whch do not produce the charge separation if we intend to simulate a neutral plasma. The purpose of the present work is to propose new methods of initially loading particles that are applicable to a neutral plasma with arbitrary density and temperature profiles. Some applications to actual simulations are also given.

2. Modified Guiding Center Loading

Let us consider an electrostatic plasma in a constant external magnetic field $\mathbf{B}_0$ along the z-axis. We assume nonuniformity exists only in the x-direction (slab geometry). The extension to the case where a plasma is nonuniform in the xy-plane, however, is straightforward for the following discussion. As is well known, an equilibrium distribution $f(x, \mathbf{v})$ with no drift velocity along the magnetic field is usually given by

$$f(x, \mathbf{v}) = N(x + v_y/\Omega)\left[\frac{m}{2\pi T(x + v_y/\Omega)}\right]^{3/2} \exp\left[-\frac{mv^2}{2T(x + v_y/\Omega)}\right], \tag{1}$$

where m and Ω represent the mass and the cyclotron frequency, $v = |\mathbf{v}|$, and $N(x)$ and $T(x)$ can be thought of the density and the temperature distributions of the guiding centers located at $x_g = x + v_y/\Omega$. It is to be noted that the actual particle density, $n(x)$, is not equal to $N(x)$ but is given by

$$n(x) = \int f(x, \mathbf{v})\, d\mathbf{v}, \tag{2}$$

because the actual position of a particle is separated from its guiding center by its Larmor radius. As discussed in the Introduction, the charge neutrality condition for a simulated plasma is not satisfied if the initial particle loading follows the usual condition, $-q_e N_e(x) = q_i N_i(x)$, where $N_\alpha(x)$ and q_α represent the guiding center density and the charge for the species α (i = ion and e = electron). For simplicity we consider the two-species plasma. Note that the species indices are neglected in this paper, if possible. The initial particle loading for realizing this condition will be called the guiding center loading (GCL). It is necessary to determine the guiding center

density $N_\alpha(x)$ in order for the actual charge neutrality, $-q_e n_e(x) = q_i n_i(x)$, to be satisfied.

Before describing methods free of the charge separation, let us derive an analytical relation between $n(x)$ and $N(x)$. Carrying out integrations with respect to v_x and v_z in Eq. (2), we obtain easily

$$n(x) = \int_{-\infty}^{+\infty} N(x + v_y/\Omega) \left[\frac{m}{2\pi T(x + v_y/\Omega)}\right]^{1/2} \exp\left[-\frac{mv_y^2}{2T(x + v_y/\Omega)}\right] dv_y. \tag{3}$$

Assuming periodicity of $N(x)$ and $T(x)$ with period L, we can rewrite Eq. (3) in a Fourier series,

$$n(k) = \frac{1}{L}\int_0^L n(x)\, e^{-ikx}\, dx, \tag{4}$$

$$n(x) = \sum_k n(k)\, e^{ikx}, \tag{5}$$

where $k = 2\pi j/L$ and j is an integer. From Eqs. (3) and (4), $n(k)$ is given by

$$n(k) = \frac{1}{L}\int_0^L dx \int_{-\infty}^{+\infty} dv_y\, N(x + v_y/\Omega)\left[\frac{m}{2\pi T(x + v_y/\Omega)}\right]^{1/2} \times \exp\left[-\frac{mv_y^2}{2T(x + v_y/\Omega)}\right] e^{-ikx}. \tag{6}$$

Now we carry out the integration with respect to v_y, so that we have

$$n(k) = \frac{1}{L}\int_0^L dx\, N(x) \exp\left[-\frac{k^2}{2m\Omega^2}\, T(x)\right] e^{-ikx}, \tag{7}$$

or

$$\tilde{n}(k) = \frac{1}{L}\int_0^L dx\, \tilde{N}(x) \exp\left[-\frac{1}{2}\, k^2\rho^2 \tilde{T}(x)\right] e^{-ikx}, \tag{8}$$

where $n(x) = n_0 \tilde{n}(x)$, $N(x) = n_0 \tilde{N}(x)$, $T(x) = T_0 \tilde{T}(x)$, and $\rho = (T_0/m)^{1/2}/|\Omega|$. Here, n_0 and T_0 are the average density and temperature, respectively, and ρ is the Larmor radius evaluated from T_0. The exponential term in Eq. (8) shows the finite Larmor radius effects which cause the difference between $n(x)$ and $N(x)$.

We will discuss shortly the effects of using GCL. If the average Larmor radius is sufficiently less than the characteristic length of the plasma inhomogeneity, i.e., $\rho d \ln(NT)/dx \ll 1$, the actual density $n(x)$ is approximately given by (from Eq. (8))

$$n(x) - N(x) \simeq n_0 \frac{\rho^2}{2}\frac{d^2}{dx^2}\{\tilde{T}(x)\,\tilde{N}(x)\}. \tag{9}$$

Hence, the following charge separation, $\delta Q(x) = q_i n_i(x) + q_e n_e(x)$, will result from GCL,

$$\delta Q(x) \simeq q_i n_{i0} \frac{\rho_i^2}{2} \frac{d^2}{dx^2} [\tilde{T}_i(x) \tilde{N}_i(x)], \tag{10}$$

where we have assumed $\rho_e \ll \rho_i$. The electric field E_x caused by the charge separation given by Eq. (10) yields a plasma flow, $v_y^E = -cE_x/B_0$, which is evaluated by the relation

$$v_y^E \simeq -\frac{1}{2} \frac{cT_{i0}}{q_i B_0} \frac{1}{1 + \Omega_i^2/\omega_{pi}^2} \frac{d}{dx} [\tilde{T}_i(x) \tilde{N}_i(x)], \tag{11}$$

where ω_{pi} is the ion plasma frequency and the reduction of the electric field due to polarization effects of the plasma has been included by the factor $(1 + \omega_{pi}^2/\Omega_i^2)^{-1}$. On the other hand, the diamagnetic velocity for the species α is

$$v_{\alpha y}^D \simeq \frac{cT_{\alpha 0}}{q_\alpha B_0} \frac{1}{\tilde{N}_\alpha(x)} \frac{d}{dx} [\tilde{N}_\alpha(x) \tilde{T}_\alpha(x)]. \tag{12}$$

We see tat v_y^E and $v_{\alpha y}^D$ are quantities of the same order for the usual parameters $(\Omega_i^2/\omega_{pi}^2 \ll 1)$.

Now let us show how to determine $\tilde{N}(x)$ so that the actual neutrality condition, $-q_e n_e(x) = q_i n_i(x)$, is satisfied. We denote such $\tilde{N}(x)$ by $\tilde{N}^M(x)$. Further, let $\tilde{N}(x)$ represent the conventional guiding center density $(-q_e N_e(x) = q_i N_i(x))$. The methods of realizing $\tilde{N}^M(x)$ in particle simulations will be referred to as modified guiding center loadings (MGCL).

If a plasma is uniform in temperature, Eq. (7) can be easily integrated to be $n(k) = \exp(-\frac{1}{2}k^2\rho^2) N(k)$. It is clear that if, instead of $N(k)$, a modified guiding center distribution $N^M(k)$ is chosen as $N^M(k) = \exp(\frac{1}{2}k^2\rho^2) N(k)$, i.e.,

$$N^M(x) = \sum_k \exp(\tfrac{1}{2}k^2\rho^2) N(k) e^{ikx}, \tag{13}$$

the actual density $n(x)$ becomes equal to $N(x)$. Consequently charge neutrality can be fulfilled everywhere. It is to be noted that this method establishes the charge neutrality condition without the assumption $\rho(d \ln n/dx) \ll 1$. We can construct an arbitrary density distribution as long as the right-hand side of Eq. (13) converges.

If a plasma has a nonuniform temperature, the problem becomes more complicated because Eq. (8) becomes coupled equations for different k modes. Here we show two methods. With the first method we obtain $\tilde{N}^M(x)$ so that $\tilde{n}(x) = \tilde{N}(x)$. It is equivalent to solving the following equations for $N^M(k)$,

$$\tilde{N}(k) = \sum_{q=-\infty}^{+\infty} G_{k,q} \tilde{N}^M(k-q), \tag{14a}$$

$$= \sum_{q=-\infty}^{+\infty} G_{k,k-q} \tilde{N}^M(q), \tag{14b}$$

where the $G_{k,q}$'s are given by

$$\exp[-\tfrac{1}{2}k^2\rho^2\tilde{T}(x)] = \sum_q G_{k,q} \exp(iqx). \tag{15}$$

It is to be noted that the truncation for large q in Eq. (15) is not safely justified because, for $k\rho \gtrsim 1$, the q-spectrum band width of $G_{k,q}$ is about $(k\rho)^2$ times as broad as that of $\tilde{T}(q)$. However, for $(k\rho)^2\, \tilde{T}_{\min} \gg 1 (0 < \tilde{T}_{\min} < 1)$, where $\tilde{T}_{\min}$ is the minimal normalized temperature, $G_{k,q}$ converges uniformly to zero for large k regardless of the value of q. Hence we can truncate Eq. (14b) for finte k and q; in general, $\tilde{N}^{\mathrm{M}}(q)$ can be obtained as a numerical solution of linear equations.

The second method is simpler than the first, but, strictly speaking, it is only applicable to the simulation where the guiding center approximation is used for electron dynamics, i.e., $n_e(x) = N_e(x)$ (full Lorentz force is used for ion dynamics). We first distribute ions in configuration space using GCL. The ion density distribution $n_i(x)$ is given by Eq. (8), or, expanding the exponential term in a Taylor series,

$$\tilde{n}_i(k) = \exp(-\tfrac{1}{2}k^2\rho_i^2) \sum_{n=0}^{\infty} \frac{(\frac{1}{2}k^2\rho_i^2)^n}{n!} H_n(k), \tag{16}$$

where

$$H_n(k) = \frac{1}{L}\int_0^L \tilde{N}_i(x)[1 - \tilde{T}_i(x)]^n\, e^{-ikx}\, dx. \tag{17}$$

The function $H_n(k)$ is obtained in order from $H_0(k) = \tilde{N}_i(k)$ and $\tilde{T}_i(k)$ using the convolution

$$H_n(k) = \sum_{q=-\infty}^{+\infty} H_{n-1}(k-q)[\delta_{q,0} - \tilde{T}_i(q)], \tag{18}$$

where $\delta_{q,0}$ is the Kronecker delta. The guiding center distribution of electrons is chosen as $N_e^{\mathrm{M}}(x) = -q_i/q_e n_i(x)$, where $n_i(x)$ is the ion density obtained from Eqs. (16)–(18). It is clear that this method guarantees the charge neutrality condition for the simulation plasma we are considering.

To end this section, we emphasize that we can simulate the neutral plasma which is nonuniform in both density and temperature without the assumption that the inhomogeneous scale of the plasma is much larger than the ion Larmor radius, by using one of the methods mentioned above.

3. Applications to Computer Simulations

Here we present a few applications of MGCL to actual particle simulations. The results using GCL are also described to make clear the difference between the methods.

3.1. *The Case of Nonuniform Density*

We first applied MGCL to the simulation of the drift wave instability driven by a density gradient. We used the electrostatic two-and-a-half-dimensional dipole expansion code [3] with a static magnetic field slightly tilted from the z-direction in the y-direction. The plasma is bounded by conducting walls at $x = 0$ and $x = L_x$ at which the electrostatic potential is zero. Method I of Ref. [4], which is guiet and produces no numerical surface instability, is used for particle reflection at the walls. Periodic boundary conditions are used in the y-direction. The density distribution is chosen as

$$\tilde{N}(x) = 1 - \varepsilon \tanh[(x - x_0)/l], \tag{19}$$

with $\varepsilon = 0.764$, $l = 7.64$ and $x_0 = 32$, where lengths are normalized by a grid spacing Δ. The plasma is uniform in temperature. The full dynamics of electrons and ions are followed. The parameters are: system size, $L_x \times L_y = 64 \times 32$; number of particles, $N_e = N_i = 16{,}384$; particle size, $a = 1.5$; time step, $\omega_{pe}\Delta t = 0.4$; $m_i/m_e = 25$; $\Omega_e/\omega_{pe} = 2$; electron Debye length, $\lambda_{De} = 2$; $T_e/T_i = 4$; angle between the magnetic field and the z-axis, $\theta = 1.5°$.

Figure 1a shows the spatial profile of the $k_y = 0$ mode of the electrostatic potential at $\omega_{pe}t = 58$ before instability sets in. With GCL, a large $k_y = 0$ mode appears as predicted in the previous section. Asymmetry in the potential profile comes from the difference in the reduction of the electric field due to polarization effects which are proportional to the density. The ratio of the maximum density to the minimum density is 7.47, which is consistent with asymmetry of the potential. On the other hand, with MGCL, the $k_y = 0$ mode is almost eliminated. Figure 1b shows the spatial profile of the ion flux. The solid curve represents the theoretical prediction for the diamagnetic flow with MGCL (see the Appendix), which is (quite accidentally) the same as the prediction of the local theory. The reduction of the ion flux measurement with GCL from the theory is mainly due to $E \times B$ drifts produced by the potential presented in Fig. 1a. With MGCL, the measured ion flux agrees very well with the

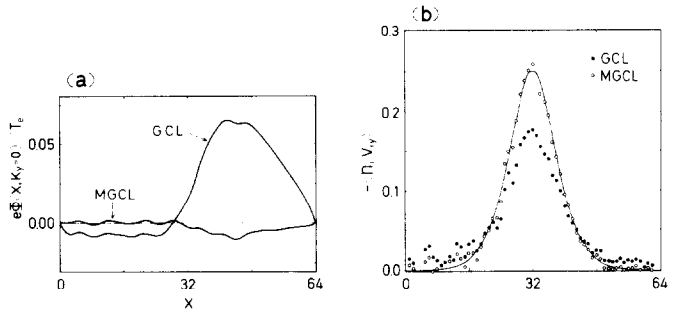

FIG. 1. Spatial profiles of (a) the electrostatic potential for the $k_y = 0$ mode and of (b) the ion flux in the y-direction. The density profile is given by Eq. (21). The solid curve in (b) represents the theoretical prediction for the diamagnetic flux with MGCL.

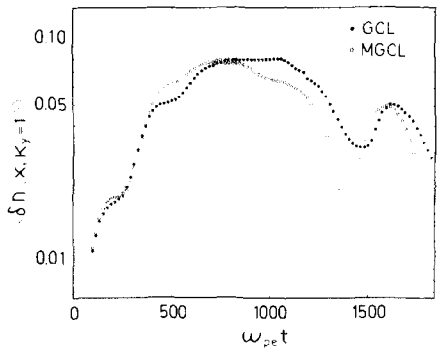

FIG. 2. Temporal evolution of the $k_y = 2\pi/L_x$ mode of the density perturbation, averaged over $0 \leqslant x \leqslant L_x$.

theoretical curve. Therefore, Fig. 1 shows that MGCL works satisfactorily, as we expected.

In Fig. 2, we illustrate the temporal evolution of the $k_y = 2\pi/L_x$ mode of the density perturbation which is averaged over $0 \leqslant x \leqslant L_x$. This mode corresponds to the most unstable drift wave mode. An appreciable difference between the results with GCL and MGCL is clearly observed. An especially drastic change occurs in the nonlinear stage of the instability ($\omega_{pe}t \gtrsim 700$). Figure 2 indicates the significance of properly treating the $k_y = 0$ mode in the drift wave simulation as well as the importance of the initial conditions.

3.2. *The Case of Nonuniform Temperature*

For the second example, we consider the temperature profile given by

$$\tilde{T}(x) = 1 - \varepsilon_T \cos\left(\frac{2\pi x}{L}\right) \qquad (\varepsilon_T < 1). \tag{20}$$

This example is of practical importance because it applies to the simulation of the anomalous heat diffusion phenomena due to convective modes or wave transport, etc. Here we use the first method described in Section 2 for the nonuniform temperature case. For this temperature profile, the matrix $G_{k,q}$ in Eq. (14) is expressed as

$$G_{k,q} = \exp(-\tfrac{1}{2}k^2\rho^2)\, I_n(\tfrac{1}{2}\varepsilon_T k^2\rho^2), \tag{21}$$

where $k = 2\pi m/L$, $q = 2\pi n/L$ (m, n: integer) and I_n is the modified Bessel function of the nth order. If the plasma density $n(x)$ is uniform, Eq. (14b) reduces to the form

$$\delta_{m,0} = I_m(\alpha m^2) + \sum_{n=1}^{\infty} [I_{m-n}(\alpha m^2) + I_{m+n}(\alpha m^2)]\, N_n^M \qquad (m \geqslant 0), \tag{22}$$

where $N_n^M = N^M(q)$ and $\alpha = \frac{1}{2}\varepsilon_T(2\pi\rho/L)^2$; the relation $N_n^M = N^M{}_n$ is assumed. The coefficients N_n^M are determined from the solution of Eq. (22).

This example was applied to the simulation with GCL and MGCL. We used a two-dimensional code with a static magnetic field in the z-direction. Periodic boundary conditions were used both in the x- and y-directions. Only electrons were followed; ions are assumed to be a charge neutralizing background. The parameters are: $N_e = 65{,}536$; $L_x \times L_y = 64 \times 64$ $(L_x = L)$; $a = 1.0$; $\lambda_{De} = 2.0$; $\varepsilon_T = 0.5$; $\Omega_e/\omega_{pe} = 0.5$; $\omega_{pe}\Delta t = 0.2$. We get $\alpha = 3.855 \times 10^{-2}$ $(\ll 1)$ for these parameters. The first mode, N_1^M, is evaluated as

$$N_1^M = -I_1(\alpha)/(I_0(\alpha) + I_2(\alpha)) \simeq -\tfrac{1}{2}\alpha = -1.927 \times 10^{-2}$$

in the first approximation and N_m^M $(m \geqslant 2)$ is the higher order quantity of α. Therefore the only N_1 $(=N_{-1})$ mode is sufficient to make the density uniform in the present simulation. (The N_m's obtained from the numerical calculation of Eq. (22) are $N_1 = -1.924 \times 10^{-2}$, $N_2 = -1.457 \times 10^{-3}$, $N_3 = -3.008 \times 10^{-4}$,....) Namely, $N^M(x) = 1 - \alpha \cos(2\pi x/L)$. Of course for $\alpha \simeq 1$, it is possible to obtain N_n^M strictly by the numerical calculation.

Figure 3 shows the spatial profiles of the electrostatic potential ($k_y = 0$ mode) and of the macroscopic velocity in the y-direction. With GCL, we see in Fig. 3a a sinusoidal potential being built up, the magnitude of which agrees very well with the prediction in Section 2. We also observe in Fig. 3b that, with GCL, the macroscopic velocity in the y-direction is reduced by a factor of 2 from the theoretical curve for the diamagnetic velocity given by the local theory. This is because the $E \times B$ drift velocity caused by the potential shown in Fig. 3a is in the direction opposite to that of the diamagnetic velocity. The reduction factor is consistent with the estimate in Section 2. However, we detect no appreciable potential using MGCL (Fig. 3a), and hence the macroscopic velocity in Fig. 3b almost agrees with the theoretical curve. We can conclude that MGCL works satisfactorily, as we had expected. This method has been used in simulations to study cross-field heat transport due to convective cell modes [5] and high frequency waves [6].

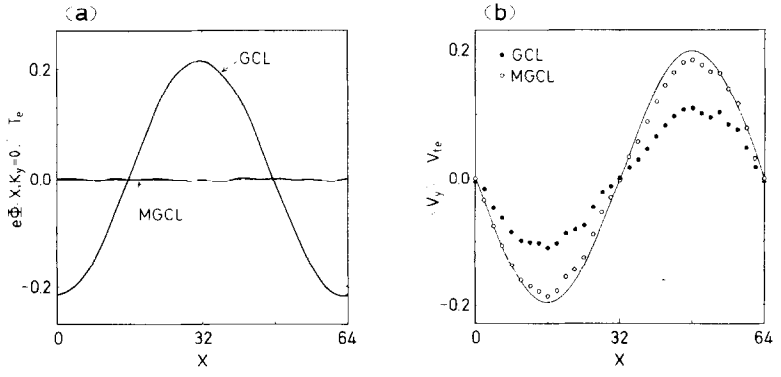

FIG. 3. Spatial profiles of (a) the electrostatic potential for the $k_y = 0$ mode and of (b) the macroscopic electron velocity in the y-direction, for the case of a single sinusoidal temperature profile. A solid curve represents the prediction of the local theory.

The extension of MGCL to the more general case, in which gradients exist both in the x- and y-directions, is quite straightforward. For example, when the temperature profile is uniform, the modified guiding center distribution $N^{M}(x, y)$ is given by

$$N^{M}(x, y) = \sum_{k_x, k_y} \exp[\tfrac{1}{2}\rho^2(k_x^2 + k_y^2)]\, N(k_x, k_y) e^{ik_x x + ik_y y}, \tag{23}$$

where $k_x = 2\pi m/L_x$ and $k_y = 2\pi n/L_y$ (m, n: integers). The other generalization is to the case where there is magnetic shear in the x-direction. If the magnetic field is expressed as $\mathbf{B} = (0, B_y(x), B_0)$ (usually $B_y(x)$ is taken to be $B_0 x/L_s$, where L_s is the shear length), the situation is simple because the canonical momentum in the y-direction is conserved. Equation (1) gives the equilibrium distribution even in this case ($n = n(x)$; $T = T(x)$). Then MGCL can be used without any change. For magnetic shear of the type $\mathbf{B} = (0, B_\theta(r), B_z)$ in the cylindrical coordinates, with the assumption that $n = n(r)$ and $T = T(r)$, the same argument prevails because the canonical angular momentum P_θ is conserved. MGCL can be also applied to this case without any change by transforming the results from Cartesian coordinates to cylindrical coordinates. Initial particle loading schemes which do not yield a charge separation for more complicated geometries of the magnetic field, including toroidicity, will be a future problem.

Appendix: Derivation of $v_y(x)$

The flux density is determined as

$$\Gamma_y(x) = \int v_y f(x, \mathbf{v})\, d\mathbf{v}, \tag{A1}$$

where $f(x, \mathbf{v})$ is given by Eq. (1) and $\Gamma_x(x) = \Gamma_z(x) = 0$. Following the method described in Section 2, we obtain

$$\Gamma_y(k) = ik \frac{n_0 T_0}{m\Omega} \int_0^L dx\, \tilde{T}(x)\, \tilde{N}(x) \exp(-\tfrac{1}{2}k^2\rho^2 \tilde{T}(x) - ikx). \tag{A2}$$

For the case of $\tilde{T}(x) = 1$, Eq. (A2) reduces to

$$\Gamma_y(k) = ik \frac{cT_0}{qB_0} \exp(-\tfrac{1}{2}k^2\rho^2)\, N(k). \tag{A3}$$

Carrying out the inverse transformation we have for the diamagnetic velocity,

$$v_y(x) = \frac{\Gamma_y(x)}{n(x)} = \frac{cT_0}{qB_0} \frac{1}{n(x)} \frac{dn(x)}{dx}, \tag{A4}$$

where $n(x)$ is the actual density. With MGCL, $N(k)$ is replaced by $N^{M}(k) = \exp(\frac{1}{2}k^2\rho^2)\, N(k)$; hence $n(k) = N(k)$ and we have

$$v_y(x) = \frac{cT_0}{qB_0} \frac{1}{N(x)} \frac{dN(x)}{dx}. \tag{A5}$$

This expression is the same as that given by the local theory where the approximation $\rho_0/L_G \ll 1$ ($L_G^{-1} = d \ln n(x)/dx$) is used. When $T(x)$ is not constant, we cannot obtain such a simple and exact relation as Eq. (A5).

ACKNOWLEDGMENTS

The authors gratefully acknowledge the helpful discussions and suggestions of Dr. H. Sanuki and Dr. Y. Ohsawa. They are also grateful to Dr. J. Van Dam for his critical reading of this manuscript and to the members of the computer center of the Institute of Plasma Physics, Nagoya University, for their assistance with the computer simulations.

REFERENCES

1. C. Z. CHENG AND H. OKUDA, *Phys. Rev. Lett.* **38** (1977), 708.
2. G. SCHMIDT, "Physics of High Temperature Plasmas," Chap. 8, p. 292, Academic Press, New York/London, 1966.
3. W. L. KRUER, J. M. DAWSON, AND B. ROSEN, *J. Comput. Phys.* **13** (1973), 114.
4. H. NAITOU, S. TOKUDA, AND T. KAMIMURA, *J. Comput. Phys.* **33** (1979), 86.
5. H. NAITOU, T. KAMIMURA, AND J. M. DAWSON, *J. Phys. Soc. Japan* **46** (1979), 258.
6. H. NAITOU, *J. Phys. Soc. Japan* **48** (1980), 608.